Image Reconstruction in Low-Field MRI

A Super-Resolution Approach

Delft University of Technology

Merel de Leeuw den Bouter

June 14, 2017

MRI scanners

MRI scanners

- Big
- Very expensive
- Problematic in developing countries

Hydrocephalus in the developing world

- Hydrocephalus
  - 400.000 newborns per year
  - 79% in developing countries
  - Limited or no access to required healthcare

Hydrocephalus in the developing world

- Hydrocephalus
  - 400.000 newborns per year
  - 79% in developing countries
  - Limited or no access to required healthcare
- Goal: develop low-cost, portable MRI scanner

Partners

- LUMC
- Pennsylvania State University
- Mbarara University of Science and Technology
- CURE Children's Hospital of Uganda

Outline

How does MRI work?

- Human body: $\sim$ 62% hydrogen atoms
- H-density $\Rightarrow$ intensity

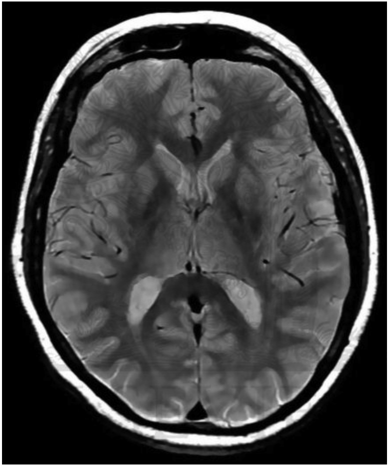

How does MRI work?

- Spin
- Random directions
- $B_0 \Rightarrow$ net magnetic moment
- Radiofrequency pulse
- Induces signal

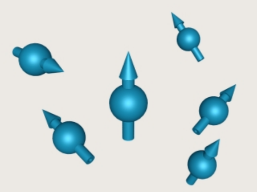

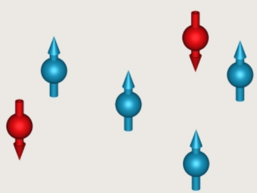

TU Delft

Conventional vs low-field MRI

Conventional MRI

- Superconducting magnets
- Strong, homogeneous magnetic field
- High signal-to-noise ratio
- Fourier Transform

$$S(t) = \iint\limits_{\text{object}} I(x, y) e^{-i(\gamma G_x t x + \gamma G_y T_{pe} y)} \, dx \, dy$$

TU Delft

Conventional vs low-field MRI

Conventional MRI

- Superconducting magnets
- Strong, homogeneous magnetic field
- High signal-to-noise ratio
- Fourier Transform

Low-field MRI

- Permanent magnets
- Weaker magnetic field with inhomogeneities
- Low signal-to-noise ratio

$$S(t) = \iint_{\text{object}} I(x,y)\omega(x,y)e^{-t/T_2^*(x,y)}e^{-i\gamma\Delta B(x,y)}\,dx\,dy$$

TU Delft

Low-field MRI

$$S(t) = \iint\limits_{\text{object}} I(x,y)\omega(x,y)e^{-t/T_2^*(x,y)}e^{-i\gamma\Delta B(x,y)}\,dx\,dy$$

Low-field MRI

$$S(t) = \iint_{\text{object}} I(x,y)\omega(x,y)e^{-t/T_2^*(x,y)}e^{-i\gamma\Delta B(x,y)}\,dx\,dy$$

$$\xrightarrow{\text{discretize}}$$

TU Delft

Low-field MRI

$$S(t) = \iint_{\text{object}} I(x,y)\omega(x,y)e^{-t/T_2^*(x,y)}e^{-i\gamma\Delta B(x,y)}\,dx\,dy$$

$$\xrightarrow{\text{discretize}}$$

$$\mathbf{s} = W\mathbf{x}$$

TUDelft

Low-field MRI

$$S(t) = \iint\limits_{\text{object}} I(x,y)\omega(x,y)e^{-t/T_2^*(x,y)}e^{-i\gamma\Delta B(x,y)}\,dx\,dy$$

$$\xrightarrow{\text{discretize}}$$

$$\mathbf{s} = W\mathbf{x} + \mathbf{e}$$

TU Delft

Prototype

LUMC

- Configuration of permanent magnets
- Inhomogeneities ⇒ spatial encoding

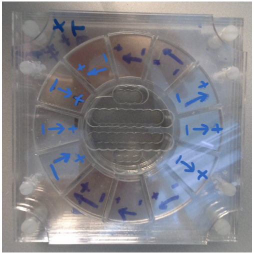

PSU

- Same components
- Inverse Fourier Transform

TUDelft

PSU prototype

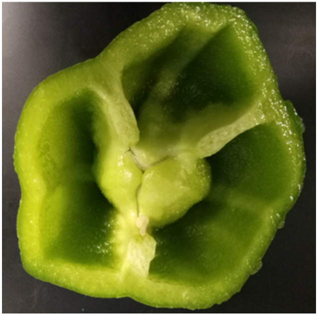

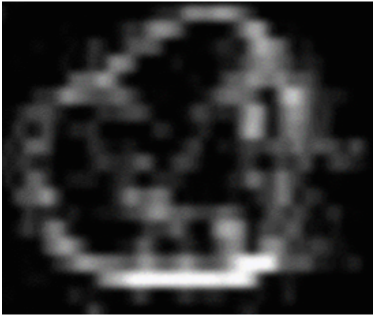

Super-resolution

- Several low-resolution images
  - Shifted
  - Rotated
- ⇒ Obtain high-resolution image

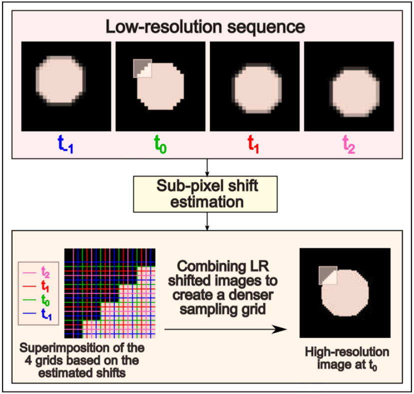

Figure: Using LR images to obtain an HR image. Source: Van Reeth et al. (2012).

Super-resolution: acquisition model

- $\mathbf{x}$: HR image
- $\{\mathbf{y}_k\}_{k=1}^{N}$: set of LR image observations

Super-resolution: acquisition model

- $\mathbf{x}$: HR image
- $\{\mathbf{y}_k\}_{k=1}^{N}$: set of LR image observations

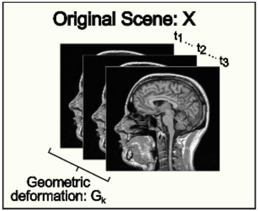

Figure: The general acquisition model. Source: Van Reeth et al. (2012).

- $\Rightarrow$ $\mathbf{x}$

Super-resolution: acquisition model

- $\mathbf{x}$: HR image
- $\{\mathbf{y}_k\}_{k=1}^N$: set of LR image observations

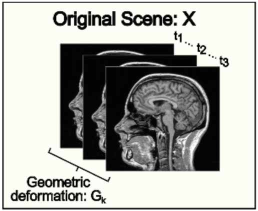

Figure: The general acquisition model. Source: Van Reeth et al. (2012).

- $\Rightarrow$ $G_k\mathbf{x}$

Super-resolution: acquisition model

- $\mathbf{x}$: HR image
- $\{\mathbf{y}_k\}_{k=1}^{N}$: set of LR image observations

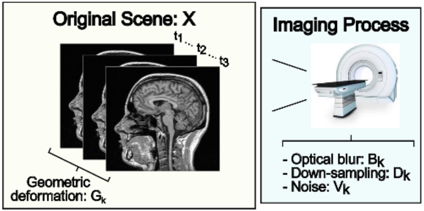

Figure: The general acquisition model. Source: Van Reeth et al. (2012).

- $\Rightarrow$ $G_k\mathbf{x}$

Super-resolution: acquisition model

- $\mathbf{x}$: HR image
- $\{\mathbf{y}_k\}_{k=1}^N$: set of LR image observations

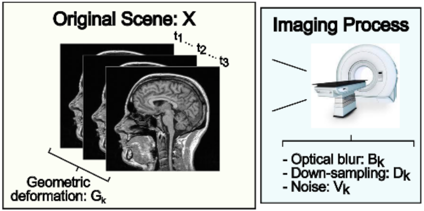

Figure: The general acquisition model. Source: Van Reeth et al. (2012).

- $\Rightarrow \qquad B_k G_k \mathbf{x}$

Super-resolution: acquisition model

- **x**: HR image
- $\{\mathbf{y}_k\}_{k=1}^{N}$: set of LR image observations

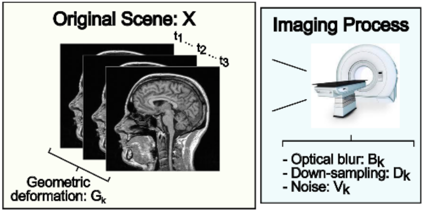

Figure: The general acquisition model. Source: Van Reeth et al. (2012).

- $\Rightarrow \qquad D_k B_k G_k \mathbf{x}$

Super-resolution: acquisition model

- $\mathbf{x}$: HR image
- $\{\mathbf{y}_k\}_{k=1}^N$: set of LR image observations

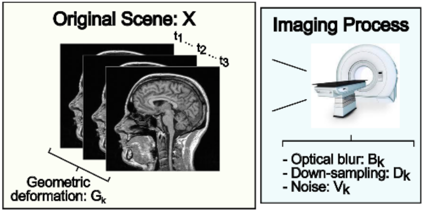

Figure: The general acquisition model. Source: Van Reeth et al. (2012).

- $\Rightarrow \qquad D_k B_k G_k \mathbf{x} + \mathbf{v}_k$

Super-resolution: acquisition model

- **x**: HR image
- $\{\mathbf{y}_k\}_{k=1}^{N}$: set of LR image observations

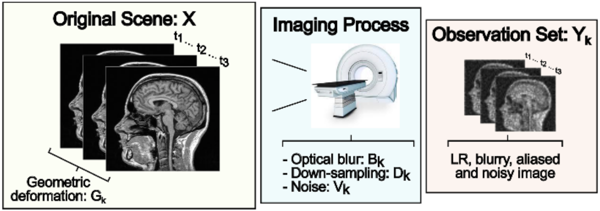

Figure: The general acquisition model. Source: Van Reeth et al. (2012).

- $\Rightarrow \mathbf{y}_k = D_k B_k G_k \mathbf{x} + \mathbf{v}_k$

Super-resolution: acquisition model

- $\mathbf{y}_k = D_k B_k G_k \mathbf{x} + \mathbf{v}_k$

Super-resolution: acquisition model

- $\mathbf{y}_k = D_k B_k G_k \mathbf{x} + \mathbf{v}_k$
- $\mathbf{y}_k = A_k \mathbf{x} + \mathbf{v}_k$

Super-resolution: acquisition model

- $\mathbf{y}_k = D_k B_k G_k \mathbf{x} + \mathbf{v}_k$
- $\mathbf{y}_k = A_k \mathbf{x} + \mathbf{v}_k$
- $\mathbf{y} = \begin{pmatrix} \mathbf{y}_1 \\ \mathbf{y}_2 \\ \vdots \\ \mathbf{y}_N \end{pmatrix}, A = \begin{pmatrix} A_1 \\ A_2 \\ \vdots \\ A_N \end{pmatrix}, \mathbf{v} = \begin{pmatrix} \mathbf{v}_1 \\ \mathbf{v}_2 \\ \vdots \\ \mathbf{v}_N \end{pmatrix}$

Super-resolution: acquisition model

- $\mathbf{y}_k = D_k B_k G_k \mathbf{x} + \mathbf{v}_k$
- $\mathbf{y}_k = A_k \mathbf{x} + \mathbf{v}_k$
- $\mathbf{y} = \begin{pmatrix} \mathbf{y}_1 \\ \mathbf{y}_2 \\ \vdots \\ \mathbf{y}_N \end{pmatrix}, A = \begin{pmatrix} A_1 \\ A_2 \\ \vdots \\ A_N \end{pmatrix}, \mathbf{v} = \begin{pmatrix} \mathbf{v}_1 \\ \mathbf{v}_2 \\ \vdots \\ \mathbf{v}_N \end{pmatrix}$
- $\mathbf{y} = A\mathbf{x} + \mathbf{v}$

Research question

Can super-resolution reconstruction yield images of better quality than direct high resolution reconstruction?

Minimization problem

- $\mathbf{y} = A\mathbf{x} + \mathbf{v}$
- $\mathbf{v}$ unknown

Minimization problem

- $\mathbf{y} = A\mathbf{x} + \mathbf{v}$
- $\mathbf{v}$ unknown
- Ill-posed problem

Minimization problem

- $\mathbf{y} = A\mathbf{x} + \mathbf{v}$
- $\mathbf{v}$ unknown
- Ill-posed problem
- $\min_{\mathbf{x}} \quad ||\mathbf{y} - A\mathbf{x}||^2$

Minimization problem

- $\mathbf{y} = A\mathbf{x} + \mathbf{v}$
- $\mathbf{v}$ unknown
- Ill-posed problem
- $\min_{\mathbf{x}} \quad ||\mathbf{y} - A\mathbf{x}||^2 + \quad \lambda||F\mathbf{x}||^2$

Minimization problem

- $\mathbf{y} = A\mathbf{x} + \mathbf{v}$
- $\mathbf{v}$ unknown
- Ill-posed problem
- $\min_{\mathbf{x}} \frac{1}{2}||\mathbf{y} - A\mathbf{x}||^2 + \frac{1}{2}\lambda||F\mathbf{x}||^2$

Minimization problem

- $\mathbf{y} = A\mathbf{x} + \mathbf{v}$
- $\mathbf{v}$ unknown
- Ill-posed problem
- $\min_{\mathbf{x}} \frac{1}{2}||\mathbf{y} - A\mathbf{x}||^2 + \frac{1}{2}\lambda||F\mathbf{x}||^2$
- λ: regularization parameter
- F: prior knowledge about $\mathbf{x}$

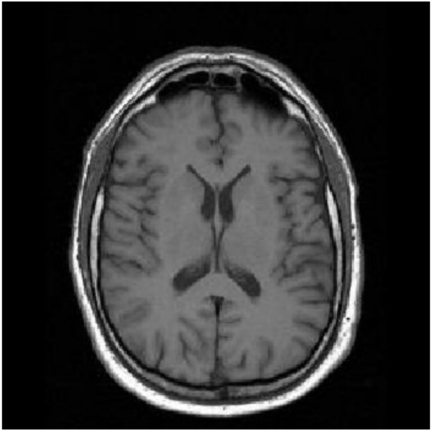

TU Delft

Different kinds of regularization

- Tikhonov:

$$\min_{x} \frac{1}{2}||\mathbf{y} - A\mathbf{x}||_2^2 + \frac{1}{2}\lambda||F\mathbf{x}||_2^2$$

- F first-order difference matrix

Different kinds of regularization

- Tikhonov:

$$\min_{x} \frac{1}{2}||\mathbf{y} - A\mathbf{x}||_2^2 + \frac{1}{2}\lambda||F\mathbf{x}||_2^2$$

- Total variation:

$$\min_{\mathbf{x}} \frac{1}{2}||\mathbf{y} - A\mathbf{x}||_2^2 + \frac{1}{2}\lambda||F\mathbf{x}||_1$$

- F first-order difference matrix

Different kinds of regularization

- Tikhonov:

$$\min_{x} \frac{1}{2}||\mathbf{y} - A\mathbf{x}||_2^2 + \frac{1}{2}\lambda||F\mathbf{x}||_2^2$$

- Total variation:

$$\min_{\mathbf{x}} \frac{1}{2}||\mathbf{y} - A\mathbf{x}||_2^2 + \frac{1}{2}\lambda||F\mathbf{x}||_1$$

- Edge-preserving
- F first-order difference matrix

TU Delft

General problem statement

- Minimization problem of the form

$$\min_{\mathbf{x}} \frac{1}{2}||\mathbf{y} - A\mathbf{x}||^2 + \frac{1}{2}\lambda||\mathbf{x}||_R^2$$

- Convex problem

General problem statement

- Minimization problem of the form

$$\min_{\mathbf{x}} \frac{1}{2}||\mathbf{y} - A\mathbf{x}||^2 + \frac{1}{2}\lambda||\mathbf{x}||_R^2$$

- Convex problem
- Sufficient condition for optimality:

$$(A^T A + \lambda R)\mathbf{x} = A^T\mathbf{y}$$

General problem statement

- Minimization problem of the form

$$\min_{\mathbf{x}} \frac{1}{2}||\mathbf{y} - A\mathbf{x}||^2 + \frac{1}{2}\lambda||\mathbf{x}||_R^2$$

- Convex problem
- Sufficient condition for optimality:

$$(A^T A + \lambda R)\mathbf{x} = A^T \mathbf{y}$$

- Conjugate gradient method

TU Delft

Conjugate gradient method

- Iterative method
- System of equations $K\mathbf{u} = \mathbf{f}$

TU Delft

Conjugate gradient method

- Iterative method
- System of equations $K\mathbf{u} = \mathbf{f}$
- Search directions $\mathbf{p}_k$ conjugate wrt K $(\mathbf{p}_k K \mathbf{p}_l = 0, \quad k \neq l)$
- $\mathbf{u}_{k+1} = \mathbf{u}_k + \alpha_k \mathbf{p}_k$
- $||\mathbf{u} - \mathbf{u}_k||_K = \min\limits_{\substack{\mathbf{v} \in \mathbf{u}_0 + \\ \text{span}\{\mathbf{p}_0, \ldots, \mathbf{p}_{k-1}\}}} ||\mathbf{u} - \mathbf{v}||_K$

Super-resolution simulations

Phantom (128 x 128 pixels)

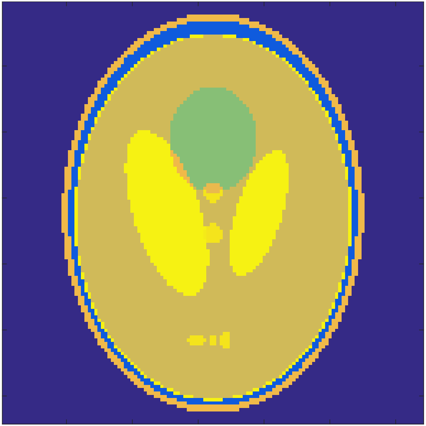

Super-resolution simulations

Shifted

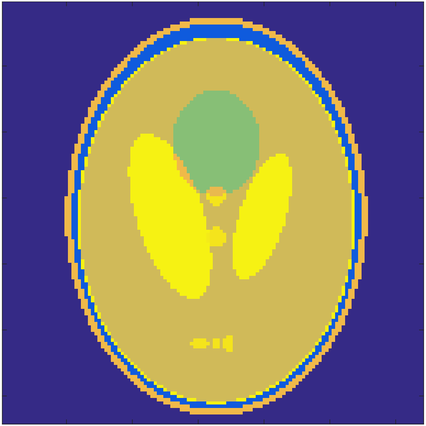

Super-resolution simulations

Blurred

Super-resolution simulations

Down-sampled

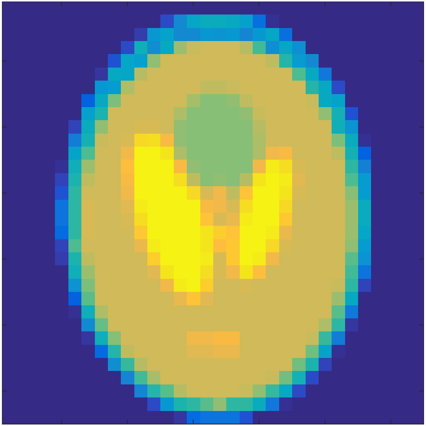

Super-resolution simulations

Noise added

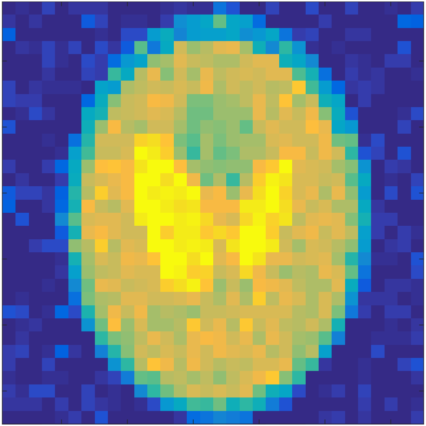

TU Delft

Super-resolution simulations

4 low resolution images (32 x 32 pixels)

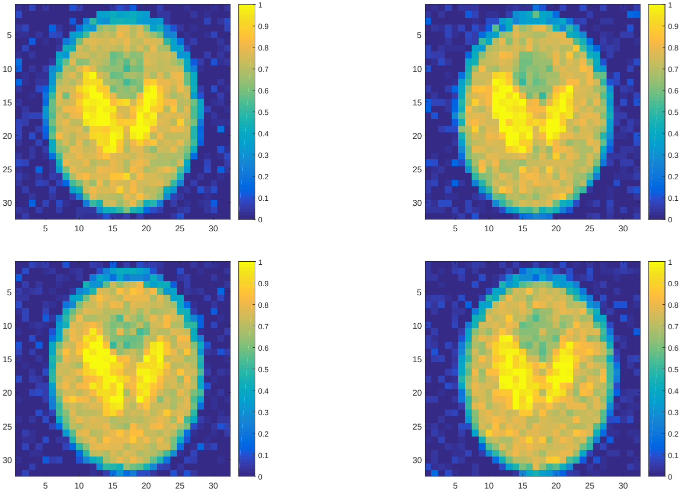

Super-resolution simulations

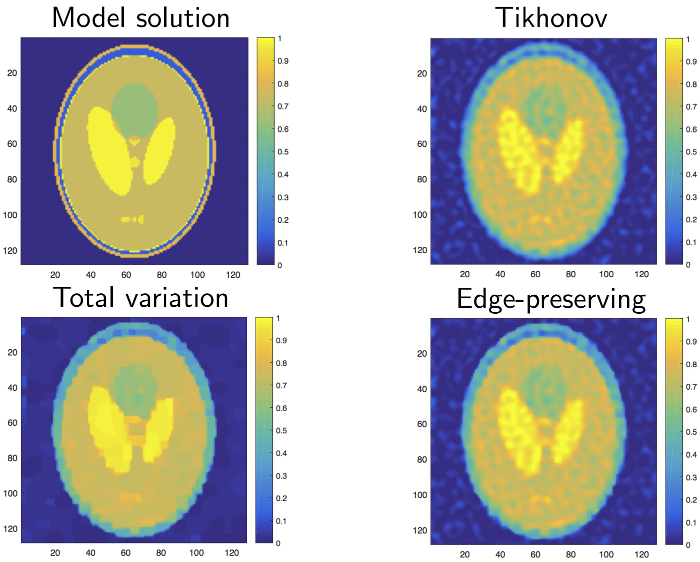

Low-field MRI simulations

- $\mathbf{s} = W\mathbf{x} + \mathbf{e}$
- Angles $0°, 10°, \ldots, 350°$
- Signal-to-noise ratios starting from 0.5

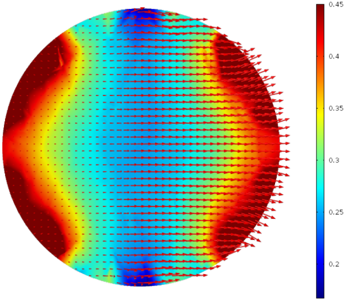

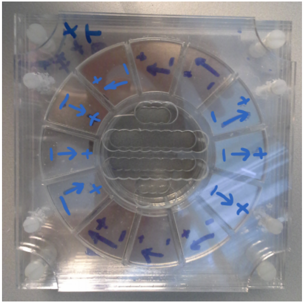

Low-field MRI simulations

Model solution

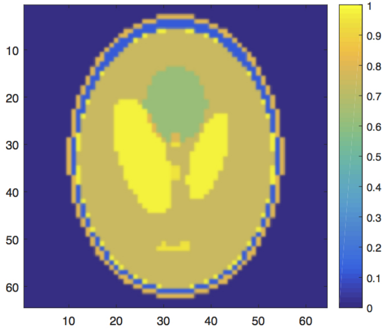

Direct HR solution (SNR = 10)

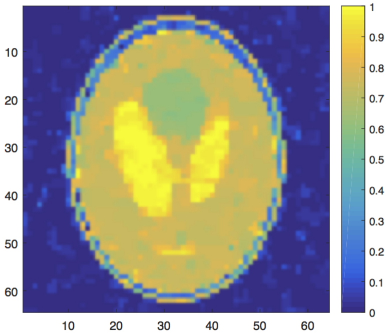

TU Delft

Low-field MRI simulations

Model solution

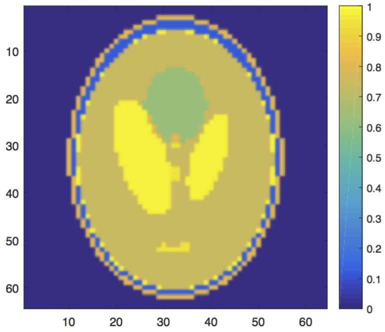

Direct HR solution (SNR = 0.5)

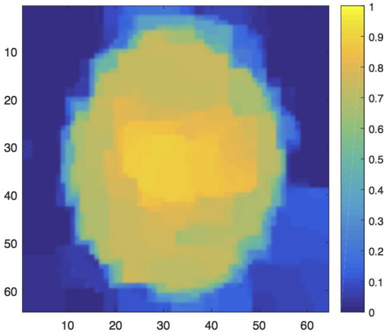

TUDelft

Low-field MRI simulations

LR images (8×8 pixels)

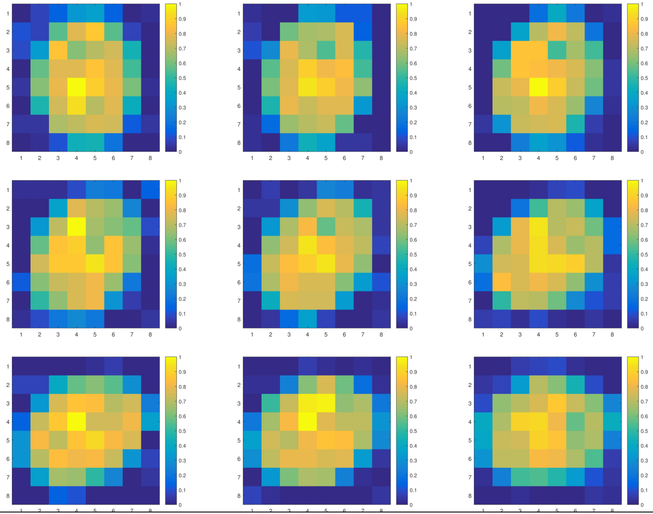

Low-field MRI simulations

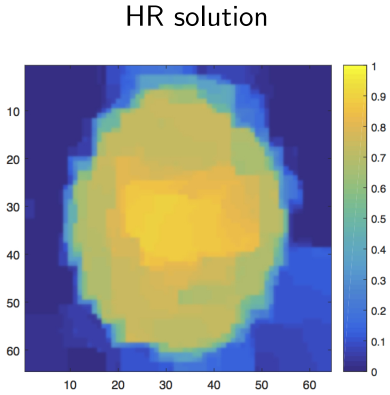

Low-field MRI simulations

SR solution

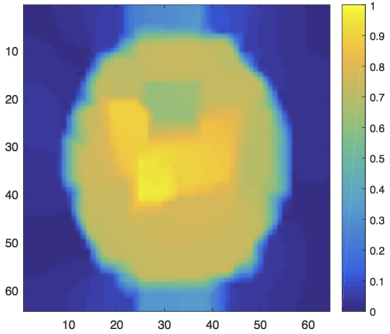

HR solution

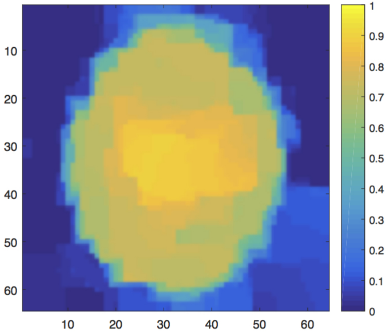

LUMC dataset

- Goal
  - Application to real data
  - Validation of the model
- 7 T MRI scanner
- Gradient in one direction
- 16 angles

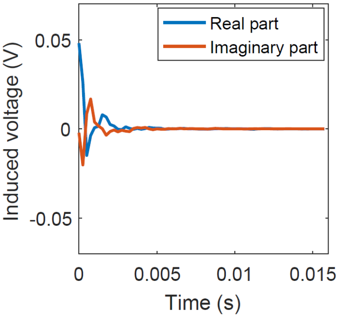

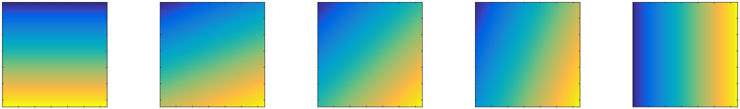

LUMC dataset

LUMC dataset

Model solution

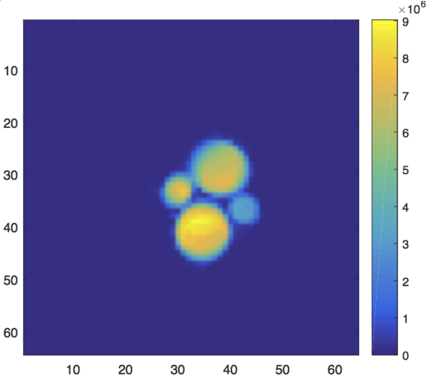

LUMC dataset

Model solution

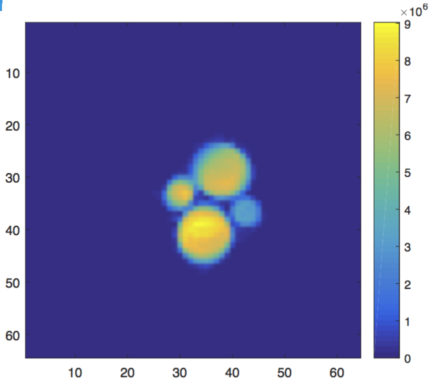

First 1D projection

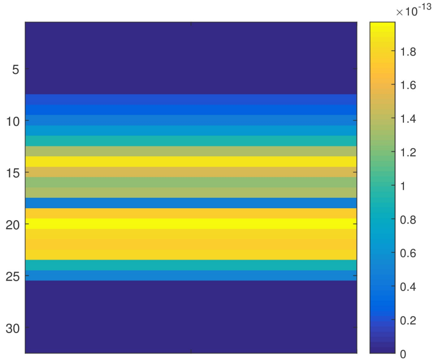

LUMC dataset

16 1D projections

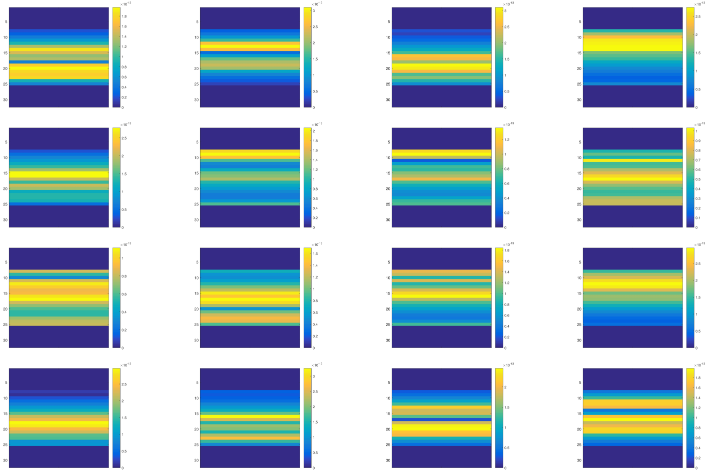

LUMC dataset

Model solution

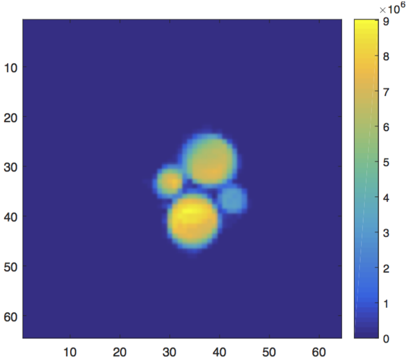

LUMC dataset

Model solution

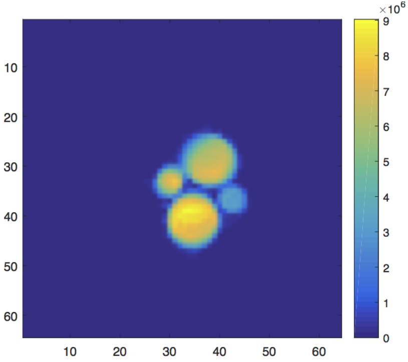

Result

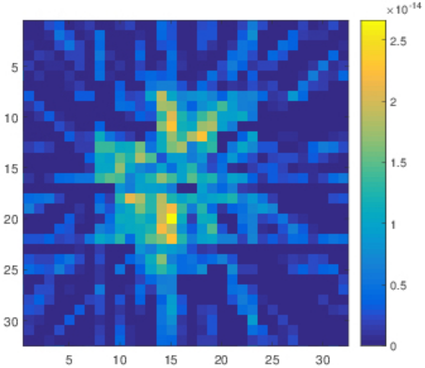

LUMC dataset

Model solution

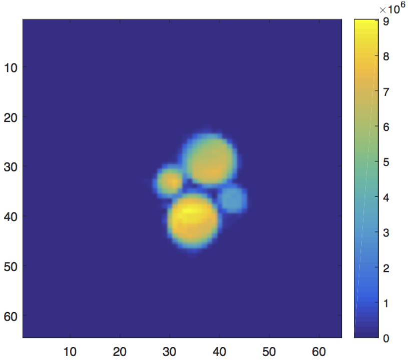

Result

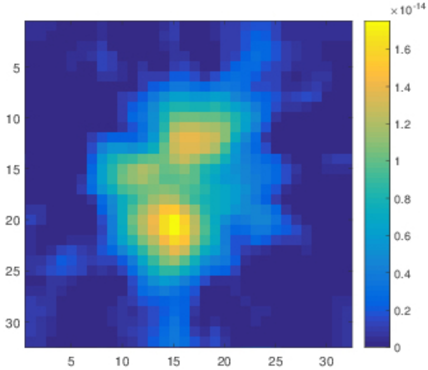

LUMC dataset

Model solution | Result

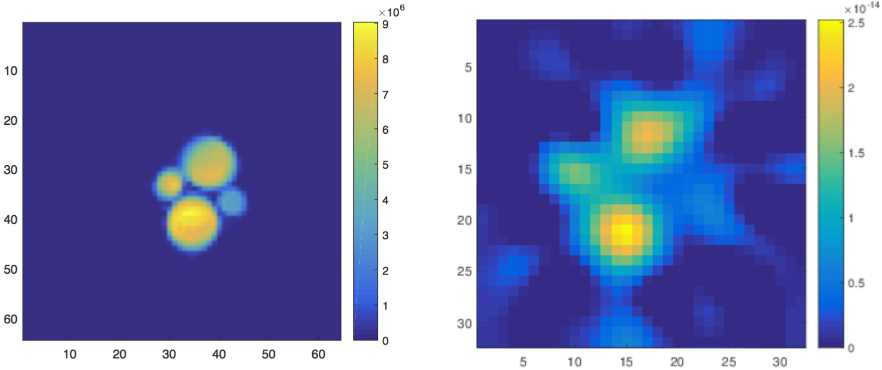

Conclusions and further research

- Conclusions
  - Super-resolution can yield better results
  - Total variation regularization
  - Validation of the measurement model

Conclusions and further research

- Conclusions
  - Super-resolution can yield better results
  - Total variation regularization
  - Validation of the measurement model
- Further research
  - Apply super-resolution to PSU data
  - New LUMC prototype
  - Measurements at LUMC with more complicated field
  - Dictionary learning

Image Reconstruction in Low-Field MRI

A Super-Resolution Approach

Delft University of Technology

Merel de Leeuw den Bouter

June 14, 2017

LUMC dataset: super-resolution

Model solution

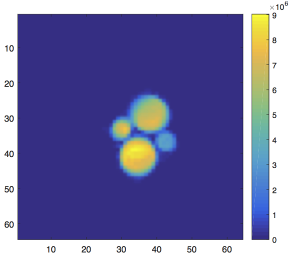

HR result

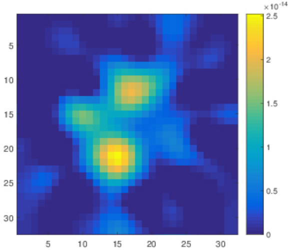

One LR image

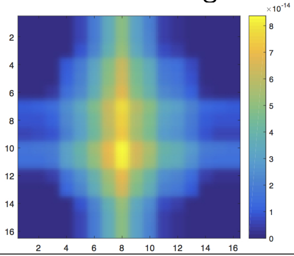

SR result

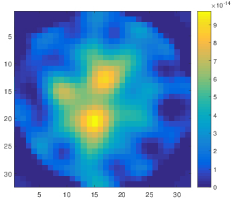

TU Delft